

## Multiangle Method for Temperature Measurement of Biological Tissues by Microwave Radiometry

Jean Montreuil and Manfred Nachman

**Abstract** — A new approach for deriving the temperature distribution in biological tissues by microwave radiometry is proposed. It consists in the measurement of the thermal radiation of the body, at a given frequency, as a function of the observation angle, for two mutually orthogonal polarizations. Theoretically, this method yields results comparable to those obtained with the multispectral method. In order to derive the relations between the body temperature and the emitted thermal signal, the biological body is modeled by a set of parallel planar layers, each characterized by constant permittivity and temperature.

### I. INTRODUCTION

Microwave radiometry is used to evaluate, noninvasively, the subcutaneous temperature distribution in biological tissues. Unfortunately, no detailed theoretical studies have been carried out, so far, on the effect of the uncertainty in the geometrical and electrical parameters of the biological tissues on the uncertainty with which the subcutaneous temperature can be determined. Moreover, different configurations of biological tissues with different temperature distributions may produce the same radiometric signal. One possible solution to this problem is to perform the measurements at several frequencies (multispectral method). The raw data have to be subsequently processed by an inversion technique, so as to yield the temperature profile inside the tissues [1]–[3]. The application of this method requires a rather complex radiometer, with an antenna matched to the body over a wide range of frequencies.

In what follows we present a new approach (multiangle method) for obtaining the temperature distribution in biological tissues by microwave radiometry. It is based on the measurement, for a fixed frequency, of the thermal signal emitted by the tissues as a function of the observation angle (Fig. 1). The proposed method consists in the following steps:

- modeling of the biological body;
- computation of the thermal signal emitted as a function of tissue parameters, observation angle, and polarization;
- retrieval of the thermal field in the tissues by the inversion of the radiometric data.

Theoretical studies of the thermal emission from layered media as a function of the observation angle and polarization have been published by Wilheit [4] for a geological structure and by Bardati [5] for a biological multilayered planar configuration. Based on these studies, we have developed a method for the retrieval of the temperature profile in a biological structure from the radiometric data. At the same time we carried out an analysis of the effect of tissue parameters on the thermal signal (for more details, see [6]).

### II. THERMAL EMISSION

The biological tissues are simulated by a structure of three planar layers, with known permittivities and thicknesses (Fig. 1).

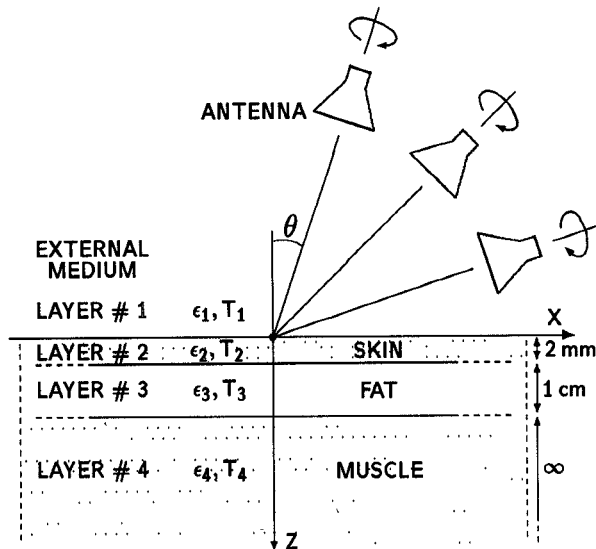


Fig. 1. Schematic diagram of the proposed multiangle method. The biological tissues are simulated here by three planar layers.

As was shown in [7], this configuration represents fairly well the actual biological structure investigated. The permittivities are taken from [8]. Assuming a constant temperature within each layer, the brightness temperature,  $T_B$ , measured by the antenna is given by

$$T_B(f, \theta, \text{pol.}) = \sum_{i=1}^4 w_i(f, \theta, \text{pol.}) T_i \quad (\text{K}) \quad (1)$$

where  $w_i$  is the weighting factor of the  $i$ th layer, calculated according to Wilheit's method [4],  $T_i$  is the temperature of the  $i$ th layer,  $f$  is the frequency, and  $\theta$  is the observation angle. The term *pol.* stands for vertical or horizontal polarization,<sup>1</sup>  $i = 1$  indicates the external medium,  $i = 2$  the skin, and so on. The weighting factor,  $w_i$ , is the percentage of energy received by the antenna from the  $i$ th layer, provided that all the layers are at the same temperature. The  $w_i$  can be determined by the reciprocity principle; they represent the fraction of energy absorbed by each layer when the antenna is in the radiating mode. To simplify the problem, Wilheit assumes that the radiation pattern of the antenna is that of an unbounded (infinite) plane wave. We analyzed the validity of this hypothesis by carrying out the calculations for a more realistic model for the antenna radiation pattern, namely assuming that the beam cross section is finite in one direction. We found that under certain conditions, these two models yield similar results (see the Appendix for further details). This justifies the use of Wilheit's model in our calculation of  $w_i$ , which requires less computing time.

In Fig. 2, the computed  $w_i$  are plotted versus the observation angle at 3 GHz (similar plots can be easily derived for other frequencies). The relative permittivity of the external medium was chosen to be  $\epsilon_{r1} = 5$  so as to ensure a better match to the body than that obtained with air. As may be inferred from Fig.

<sup>1</sup>A vertically polarized wave has its electric field in the plane determined by the propagation direction and the normal to the interfaces. In a horizontally polarized wave the electric field is parallel to the interfaces.

Manuscript received November 13, 1990; revised March 6, 1991.  
The authors are with the Department of Electrical Engineering, École Polytechnique, P.O. Box 6079, Station A, Montreal, Canada H3C 3A7.  
IEEE Log Number 9100849.

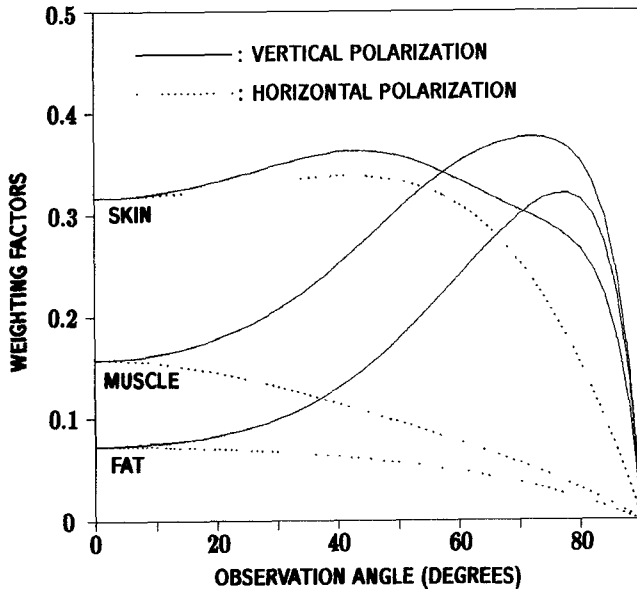


Fig. 2. Weighting factors versus observation angle; frequency = 3 GHz,  $\epsilon_{r1} = 5$ .

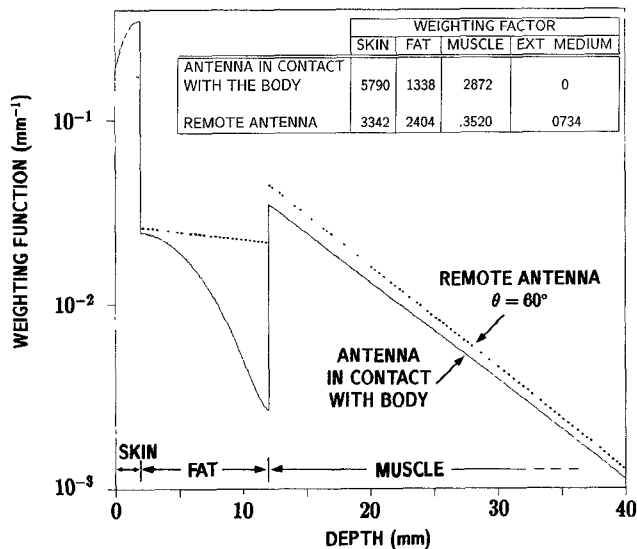


Fig. 3. Weighting function for an antenna in contact with the body and for a remote antenna ( $\epsilon_{r1} = 5$ ) at 3 GHz. The parameters used for the biological tissues are shown in Fig. 1.

2, the weighting factors present rather large variations with the observation angle (especially for the vertical polarization). This effect may be used for increasing the precision with which the temperature distribution is determined. In Fig. 3, the weighting function<sup>2</sup> of an antenna in contact with the biological body, the observation angle being  $0^\circ$  (the configuration usually employed in radiometry), is compared with the one of the antenna not in direct contact with the body. The observation angle for the latter is chosen close to the pseudo-Brewster angle.<sup>3</sup> We as-

<sup>2</sup>The weighting function represents the weighting factor of a layer of infinitesimal thickness, situated at a depth  $z$ . For example, the integral of the weighting function between the skin-fat and fat-muscle interfaces gives the weighting factor of the fat layer.

<sup>3</sup>The pseudo-Brewster angle is defined as the angle for which the reflectivity is minimum.

sumed that the antenna in contact with the body was filled with a dielectric of relative permittivity  $\epsilon_{r1} = 30$  and was perfectly matched to the body. It is seen that for the remote antenna, the weighting factor of the muscles is greater by 22% than that for the antenna in contact with the body. It may therefore be concluded that more information on deep-seated tissues can be extracted from the radiometric data supplied by the remote antenna.

### III. INVERSION PROCEDURE FOR THE TEMPERATURE OF THE LAYERS

The retrieval, from the radiometric data, of the temperatures of the layers simulating the biological tissues is performed by an inversion procedure. The linear equations (1) are solved by applying a matrix method similar to that employed by Edenhofer [9] for analyzing multispectral data. The only difference here is that our data are taken for several observation angles, instead of for several frequencies. For a given frequency and polarization,<sup>4</sup>

$$\begin{bmatrix} T_B(\theta_1) \\ T_B(\theta_2) \\ T_B(\theta_3) \\ T_B(\theta_4) \end{bmatrix} = \begin{bmatrix} w_1(\theta_1) & w_2(\theta_1) & w_3(\theta_1) & w_4(\theta_1) \\ w_1(\theta_2) & w_2(\theta_2) & w_3(\theta_2) & w_4(\theta_2) \\ w_1(\theta_3) & w_2(\theta_3) & w_3(\theta_3) & w_4(\theta_3) \\ w_1(\theta_4) & w_2(\theta_4) & w_3(\theta_4) & w_4(\theta_4) \end{bmatrix} * \begin{bmatrix} T_1 \\ T_2 \\ T_3 \\ T_4 \end{bmatrix} \quad (K)$$

$$(2)$$

where  $\theta_1$  to  $\theta_4$  are four different observation angles. By inverting the weighting factors matrix  $[W]$ , we obtain

$$[T] = [W]^{-1}[T_B] \quad (K) \quad (3)$$

where  $[T]$  and  $[T_B]$  are the vectors representing the temperatures of the layers and the brightness temperatures, respectively. For more stability, the system can be overdetermined. The inversion is carried out by the Gaussian least-squares method:

$$[T] = ([W]^* [W])^{-1} [W]^* [T_B] \quad (K) \quad (4)$$

where the asterisk indicates the transposed matrix.

The standard deviations of the temperatures of the layers,  $\sigma_{Ti}$ , are evaluated with the known relations for independent and random errors:

$$\sigma_{Ti} = \sqrt{b_{11}^2 \sigma_{TB}^2 + b_{12}^2 \sigma_{TB}^2 + b_{13}^2 \sigma_{TB}^2 + b_{14}^2 \sigma_{TB}^2} \quad (K) \quad (5)$$

where  $\sigma_{TB}$  is the standard deviation of measurement noise (usually 0.1 K), and  $b_{ij}$  are the elements of the matrix product  $([W]^* [W])^{-1} [W]^*$ .

### IV. RESULTS

Table I summarizes the standard deviations of the temperatures of the layers, which can be obtained theoretically by radiometric measurements. The data are presented here for observation angles of  $0^\circ$ ,  $20^\circ$ ,  $40^\circ$ ,  $60^\circ$ , and  $80^\circ$ , for horizontal and vertical polarizations, for  $f = 3$  GHz, and for several low-loss materials as the external medium. For the case  $\epsilon_{r1} = 30$ , data for only three observation angles ( $0^\circ$ ,  $10^\circ$ , and  $20^\circ$ ) are given because a total internal reflection occurs above  $25.7^\circ$ . Since the temperature of the external medium,  $T_1$ , can be easily found experimen-

<sup>4</sup>For simplicity, the dependence on frequency and polarization is not indicated explicitly in (2).

TABLE I  
STANDARD DEVIATIONS OF THE TEMPERATURES OF THE BIOLOGICAL TISSUES OBTAINED  
a) WITH THE MULTIANGLE METHOD (MEASUREMENTS CARRIED OUT AT A FIXED  
FREQUENCY, FOR SEVERAL OBSERVATION ANGLES, AND FOR VERTICAL AND  
HORIZONTAL POLARIZATIONS) AND b) WITH THE MULTISPECTRAL METHOD  
(MEASUREMENTS CARRIED OUT AT SEVERAL FREQUENCIES)

External Medium	Standard Deviation of the Temperature (K)		
	Skin	Fat	Muscle
a)	Air	2.1	56.7
	$\epsilon_{r1} = 2.5$	0.7	8.4
	$\epsilon_{r1} = 5$	0.32	1.3
	$\epsilon_{r1} = 30$	0.26	2.2
b)	—	0.12	1.1
			1.7

tally, we assumed it to be known, in order to reduce the number of unknown parameters.

It is seen from Table I that for relative permittivities of the external medium,  $\epsilon_{r1}$ , up to 2.5, the standard deviations are too high for most medical applications. For the other cases, they are comparable to the standard deviations derived theoretically by the multispectral method [9] for an antenna in contact with the biological body at frequencies around 3, 5, 10, and 32 GHz. The results of these calculations are also listed in Table I.

## V. DISCUSSION

From the data shown in Table I it may be concluded that, in principle, by using the proposed approach the thermal profile inside a biological body can be determined with a precision comparable to that obtained with the multispectral method. The difficulties encountered when trying to match the antenna to the biological tissues are avoided. It is also seen that higher precisions are obtained for the case of vertical polarization and with the antenna embedded in a dielectric of high permittivity.<sup>5</sup> When a remote antenna is used, the interference caused by environmental noise has to be eliminated by adequate screening. Finally, it should be emphasized that for the application of this method the values of the permittivities and thicknesses of the tissues must be known.

## VI. CONCLUSION

A new approach in microwave radiometry has been proposed. It consists in measuring the thermal radiation of the body at a given frequency, at several observation angles, and at two mutually orthogonal polarizations. This multiangle method yields results comparable to those of the multispectral method. It has also been demonstrated that for all practical purposes the radiation pattern of the antenna may be approximated by that of an unbounded plane wave.

## APPENDIX

A more realistic model than that of Wilheit [4] is used here for evaluating the weighting factors of a stratified planar medium as a function of the observation angle, for an antenna not in direct contact with the medium. Instead of approximating the radiation pattern of the antenna by an unbounded plane wave, its beam cross section is considered to be finite in one direction.

<sup>5</sup>See, for example, the solution suggested by Haslam [10].

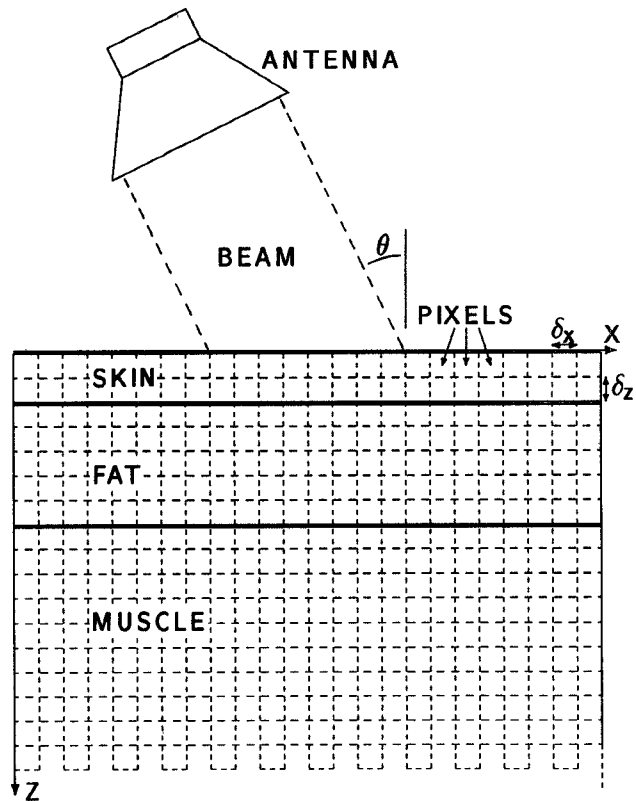


Fig. 4. Representation of the biological structure and of the antenna beam used for evaluating the weighting factors.

The weighting factors are computed for individual pixels instead of for infinite layers (see Fig. 4). They are determined using the reciprocity principle. For a given antenna position, observation angle, polarization, and frequency, we have

$$w_i = \frac{1}{2} \sigma'_i |E_i|^2 \Delta v_i P_{\text{ant}}^{-1} \quad (\text{A1})$$

$$\sigma'_i = \epsilon'' \epsilon_0 \omega \quad \left( \frac{\text{mho}}{\text{m}} \right) \quad (\text{A2})$$

where  $w_i$  is the weighting factor of the  $i$ th pixel,  $\sigma'_i$  its conductivity,  $E_i$  the electric field in the  $i$ th pixel, and  $\Delta v_i$  the volume associated with the pixel ( $\delta x \cdot \delta z \cdot 1 \text{ m}$ ).  $P_{\text{ant}}$  is the total power emitted by the antenna, and  $\omega$  is the angular frequency. The problem is to evaluate the electric field in each pixel. We developed for this purpose the procedure illustrated in Fig. 5. In

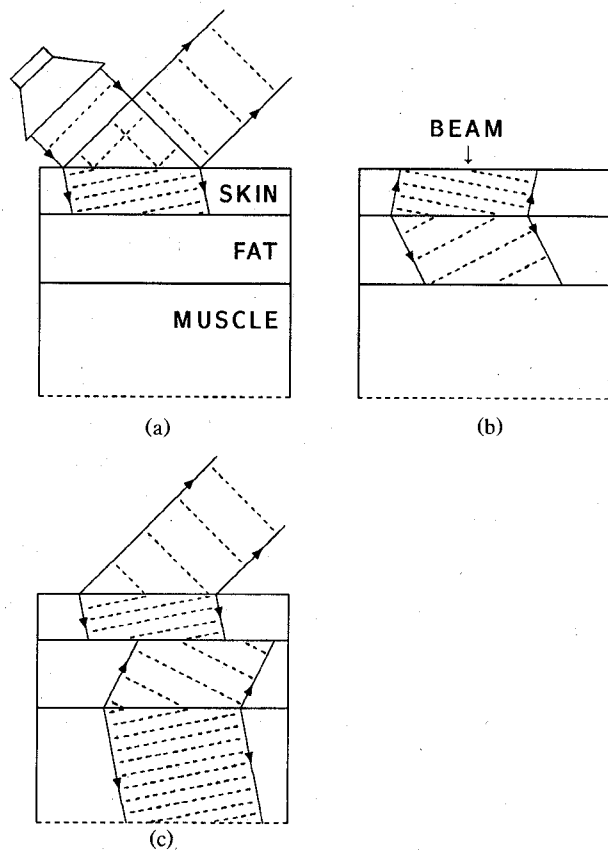


Fig. 5. Representation of the beam trajectory in a stratified medium.

(a) a microwave beam from the antenna penetrates the skin layer. The computer program calculates the electric field in each skin pixel with the well-known formulas for wave propagation. As seen in (b), part of the beam is reflected back into the skin by the skin-fat interface. The program calculates again the field in each pixel, and adds it to the previous value, taking into account the phase. In (c), the two beams indicated in (b) are again reflected and transmitted, the electric field is again calculated, and so on until its amplitude becomes smaller than a fixed value chosen by the user.

Fig. 6 gives an example of the results. In our computation, the pixel's area was  $1 \text{ mm}^2$  in the  $x-z$  plane.

The weighting factors of the different layers (obtained by adding the weighting factors of the pixels situated in the same layer) were compared with the ones obtained with Wilheit's method for the same biological structure at 3 GHz. The following conclusions may be drawn:

- As expected, the narrower the antenna beam width, the larger the difference between the data supplied by the two models.
- If the external medium is air and the beam is of minimum acceptable width ( $\frac{1}{2}\lambda_{\text{air}}$ ), then the weighting factors computed for the two models differ by 1% to 5% for the case of the vertical polarization and by 1% to 8% for the horizontal polarization. This difference depends on the observation angle.
- For  $\epsilon_{r1} = 5$ , a beam width of 5 cm ( $1.1\lambda_{\text{external medium}}$ ) and an observation angle of  $60^\circ$ , the difference for the two models is in the range from 1% to 5% for the vertical polarization.

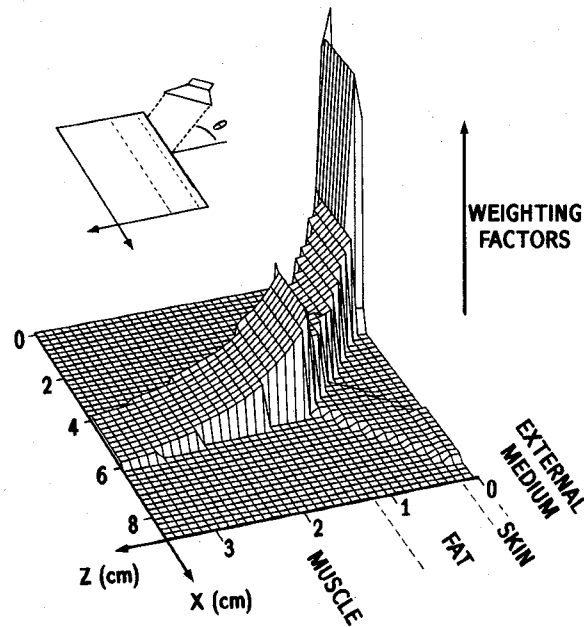


Fig. 6. Weighting factors of biological tissues in the  $x-z$  plane (observation angle =  $25^\circ$ ;  $\epsilon_{r1} = 30$ ; beam width = 2 cm;  $f = 3 \text{ GHz}$ ). Each node corresponds to the center of a pixel.

- For  $\epsilon_{r1} = 30$  and a beam width of 2 cm ( $1.1\lambda_{\text{external medium}}$ ), the weighting factors in the two models may differ by as much as 10%.

As a general conclusion it may be stated that the thicker the layers compared with the beam size, the less correct the unbounded plane wave approximation for the radiation pattern of the antenna.

#### ACKNOWLEDGMENT

The authors would like to express their gratitude to R. Archambault for his assistance with the computations.

#### REFERENCES

- [1] A. Mamouri, J. C. Van De Velde, M. Hochedez, B. Bocquet, and Y. Leroy, "Recent progress in microwave thermography," in *Proc. Eighth Annual Conf. IEEE/Eng. in Medicine and Biology Soc.*, Nov. 1986, pp. 1520-1523.
- [2] F. Bardati, M. Mongiardo, D. Solimini, and P. Tognolatti, "Biological temperature retrieval by scanning radiometry," in *IEEE MTT-S Int. Microwave Symp. Dig.*, June 1986, pp. 763-766.
- [3] Y. Hamamura, S. Mizushima, and T. Sugiura, "Non-invasive measurement of temperature-versus-depth profile in biological systems using a multiple-frequency-band microwave radiometer system," *Automedica*, vol. 8, pp. 213-232, 1987.
- [4] T. Wilheit, "Radiative transfer in a plane stratified dielectric," *IEEE Trans. Geosci. Electron.*, vol. GE-16, no. 2, pp. 138-143, April 1978.
- [5] F. Bardati and D. Solimini, "Radiometric sensing of biological layered media," *Radio Sci.*, vol. 18, no. 6, pp. 1393-1401, Nov.-Dec. 1983.
- [6] J. Montreuil, "Analyse de la méthode de mesure de température par radiométrie micro-ondes," M.Sc.A thesis, Ecole Polytechnique of Montreal, Montreal, Canada, Dec. 1989.
- [7] A. W. Guy, "Analyses of electromagnetic fields induced in biological tissues by thermographic studies on equivalent phantom models," *IEEE Trans. Microwave Theory Tech.*, vol. MTT-19, pp. 205-214, Feb. 1971.
- [8] M. A. Stuchly and S. S. Stuchly, "Dielectric properties of biological substances—Tabulated," *J. Microwave Power*, vol. 15, no. 1, pp. 19-26, Mar. 1980.

- [9] P. Edenhofer, "Electromagnetic remote sensing of the temperature profile in a stratified medium of biological tissues by stochastic inversion of radiometric data," *Radio Sci.*, vol. 16, no. 6, pp. 1065-1069, Nov. 1981.
- [10] N. C. Haslam, A. R. Gillespie, and C. G. T. Haslam, "Aperture synthesis thermography—a new approach to passive microwave temperature measurements in the body," *IEEE Trans. Microwave Theory Tech.*, vol. MTT-32, pp. 829-834, Aug. 1984.

## A Cooled 1-2 GHz Balanced HEMT Amplifier

Stephen Padin and Gerardo G. Ortiz

**Abstract**—The design details and measurement results for a cooled L-band balanced HEMT amplifier are presented. The amplifier uses commercially available packaged HEMT devices (Fujitsu FHR02FH). At a physical temperature of 12 K the amplifier achieves noise temperatures between 3 and 6 K over the 1 to 2 GHz band. The associated gain is  $\sim 20$  dB.

### I. INTRODUCTION

Cryogenically cooled high electron mobility transistor (HEMT) amplifiers have realized noise temperatures as low as the operating frequency of the amplifier expressed in GHz at frequencies up to 43 GHz [1], [2]. These amplifiers have now become the standard for radio astronomy applications. Cooled HEMT amplifiers are also used as the first IF stage in millimeter-wave superconductor-insulator-superconductor (SIS) and Schottky mixer systems. In these receivers the noise performance of the IF amplifier is very important because the mixer is usually lossy.

Most millimeter-wave receiver systems built for radio astronomy use an L-band IF amplifier with a bandwidth of  $\sim 500$  MHz and a noise temperature of  $\sim 4$  K [3], [4]. In a typical 115 GHz SIS receiver, the IF amplifier contributes  $\sim 30\%$  of the total receiver noise. A bandwidth of 500 MHz is barely enough for observations of sources with high velocity dispersion and it limits the capability of systems which are able to observe several molecular transitions simultaneously. Increasing the receiver bandwidth by using a higher frequency IF amplifier is not viable because this would increase the IF noise contribution and degrade the sensitivity of the system. Our approach to this problem has been to develop a 1-GHz-bandwidth L-band cooled HEMT amplifier.

The main problem in the design of a wideband cooled amplifier is obtaining  $s$  parameters and noise parameters for transistors at low temperatures. For this work no facilities were available for measuring low-temperature  $s$  parameters, but the HEMT noise parameters were measured at a physical temperature of 12 K. The absence of  $s$ -parameter information precluded the design of a feedback amplifier, so a balanced configuration was adopted. This has the advantage of providing a good input match even though the amplifiers in the two arms of the

balanced circuit are poorly matched. However, there are disadvantages. The loss of the input hybrid degrades the noise temperature and coupling errors in the hybrids, and differences between the amplifiers reduce the gain and result in a noise contribution from the input load. In the amplifier described here these effects degrade the noise temperature by less than 1 K.

### II. NOISE IN A BALANCED AMPLIFIER

The noise contributions in a balanced amplifier are explored in Fig. 1. Each hybrid directs a fraction,  $c$ , of the input power to the  $0^\circ$  port and the remaining power to the  $90^\circ$  port. The deviation from quadrature at the outputs is  $\theta$ . To simplify the analysis the amplifiers are assumed to have similar gains but different transfer function phases. In practice this situation can be approached by selecting similar devices and by adjusting the bias.

The power gain of the balanced amplifier (with the input terminated in a matched source and the output terminated in a matched load) is

$$G = 2gc(1 - c)(1 + \cos \phi) \quad (1)$$

where  $g$  is the power gain of each amplifier in the balanced structure and  $\phi$  is the phase difference between the amplifier transfer functions. The output noise temperature with the input terminated in a matched source at 0 K is

$$T_{\text{out}} = gT_0[(2c^2 - 2c + 1) - 2c(1 - c)\cos \phi] + gT_a \quad (2)$$

where  $T_0$  is the physical temperature of the input hybrid termination and  $T_a$  is the noise temperature of each amplifier. The first term is the contribution from the input hybrid termination and the second term represents the noise generated by the amplifiers. Note that the noise from the two amplifiers is uncorrelated. The noise temperature of the balanced amplifier is

$$T_n = \frac{T_{\text{out}}}{G} = \frac{T_0[(2c^2 - 2c + 1) - 2c(1 - c)\cos \phi] + T_a}{2c(1 - c)(1 + \cos \phi)}. \quad (3)$$

The loss of the input hybrid can be modeled as an attenuator at the amplifier input. Loss in the output hybrid affects only the overall gain (and hence the noise contribution of the next stage). With an input hybrid loss  $L$ , the noise temperature of the balanced amplifier is

$$T'_n = T_0(L - 1) + LT_n \quad (4)$$

where  $T_n$  is given by (3). As an example of what might be achieved, a balanced circuit containing amplifiers with  $T_a = 4$  K and  $\phi = 5^\circ$  and hybrids with coupling errors of 1 dB ( $c = 0.40$ ) and excess loss of 0.1 dB would have a noise temperature of 5.09 K at a physical temperature of 12 K. If the input load were at 4 K instead of 12 K the noise temperature would be 4.73 K.

### III. HEMT DEVICE NOISE PARAMETERS

Device noise parameters for this work were obtained from measurements of the noise temperatures of several single-ended amplifiers, each with a different input matching network. The same HEMT device was used for the entire set of measurements. Previous work with GaAs FET's at L-band [5] provided

Manuscript received November 29, 1990; revised February 27, 1991. This work was supported by the Caltech President's Fund and by NASA under Contract NAS7-100.

S. Padin is with the Owens Valley Radio Observatory, California Institute of Technology, Big Pine, CA 93513.

G. G. Ortiz is with the Jet Propulsion Laboratory, 4800 Oak Grove Drive, Pasadena, CA 91109.

IEEE Log Number 9100144.